

Atomic Bose-Einstein Condensates: A Model for Macroscopic Quantum Systems

D. Meschede, V. Gomer

Institut für Angewandte Physik, Universität
Bonn, Wegelerstrasse 8, D-53115 Bonn

H. Monien

Physikalisches Institut, Universität Bonn, Nuss-
allee 12, D-53115 Bonn

A novel type of macroscopic quantum system has recently become available through the experimental realization of Bose condensates from neutral atoms. We review experimental results and the elementary quantum mechanical approach and outline advanced theoretical concepts regarding finite size, potentials, dimensionality, and interactions.

Introduction: Macroscopic Quantum Systems

Quantum theory is traditionally considered and taught as a description of microscopic systems in the first place. Its precision and prediction capacity for simple physical systems such as the hydrogen atom is without precedent and has remained unchallenged for more than 70 years. On the other hand, so-called “macroscopic quantum systems” continue to draw much excitement. When we attribute “quan-

tum character” to an object, it is not only the discrete energy level structure of a system with finite dimensions. Perhaps more importantly it is the wave aspect, which allows for interference phenomena of particles with mass. Strictly speaking, any condensed sample, even a simple electron gas in a metal, belongs to this class. The classical appearance, i.e., visualization in terms of a stochastic ensemble of pointlike particles, is usually caused by a large number of degrees of freedom available for the motion of such systems, resulting in a rapid dephasing of quantum correlations at elevated temperatures. In such systems quantum interferences can safely be neglected.

The attraction of quantum systems that are called “macroscopic” is, in contrast, derived from the fact that quantum correlations of the system are important or even dominant over conventional forces such as the Coulomb interaction. Longer known examples include superconductivity and superfluidity of liquid helium. More recently a novel macroscopic quantum state of matter has been produced from a dilute gas of bosonic alkali atoms in a magnetic container, which is considered to be the first realization of a weakly interacting Bose condensate. It is common to all such systems that their lowest energy level can be described by a single macroscopic wavefunction, i.e., the ground state of this system is occupied by numerous particles. We restrict the term “macroscopic quantum state” here to this class of many-particle systems.

The first part of this overview is devoted to a naive analysis of thermodynamical properties of a bosonic quantum gas. Quantum mechanics is employed through elementary quantum statistics and through wavefunction analysis. In the second part we make a bold attempt to introduce more advanced

concepts of many-body quantum physics and field theory to a general audience.

Atomic Bose-Einstein-Condensates

Elementary Predictions

In 1925 Albert Einstein [1] showed that for an ideal Bose gas of N particles, with mass m confined in a rigid container of volume V , a macroscopic occupation of the ground state can occur at the finite temperature

$$T_c = \frac{h^2}{2\pi k_B m} \left[\frac{1}{2.612} \frac{N}{V} \right]^{2/3} \quad (1)$$

where k_B is Boltzmann's constant and h is Planck's constant. He was inspired in this work by Satyendra N. Bose [2], who had considered the problem for a gas of identical photons. This purely quantum-statistical phase transition is a consequence of the indistinguishability of bosonlike particles, and one of the rare examples of a macroscopic quantum state. This mysterious phenomenon has been known as Bose-Einstein condensation (BEC) for more than 70 years, but it has proven difficult to achieve by experimenters in its pure form. A naive way to "explain" the BEC makes use of the thermal de Broglie wavelength:

$$\Lambda = \frac{h}{\sqrt{2\pi m k T}} \quad (2)$$

We can rewrite Eq. 1 in terms of the particle number density $n = N/V$:

$$n\Lambda^3 = 2.612 \quad (3)$$

Thus the condition for Bose condensation to occur in a 3D box requires the average distance between particles $n^{-1/3}$ to be approximately equal to the de Broglie wavelength. Λ is a quantum measure for delocalization of a particle, i.e., the appearance of wavelike properties. At T_c the wave packets describing the particle begin to overlap, indicating the onset of quantum degeneracy. Add the known preference of bosons to balle and one can "understand" the effect.

The product $n\Lambda^3$ is called "phase space density." Phase space describes the configuration volume (space \times momentum) available to a given physical system. In three dimensions it is divided into quantum unit cells of volume h^3 . A unit cell can be populated by only one fermionic particle (with half integer spin) at a time but by an arbitrary number of

bosonic particles (with integer spin quantum number) constituting a "degenerate quantum system." The prediction of Einstein is a consequence of the Bose-Einstein distribution describing the occupation number N_ε of particles in an energy level ε and given by:

$$N_\varepsilon = \frac{1}{\exp\left(\frac{\varepsilon - \mu}{kT}\right) - 1} \quad (4)$$

The chemical potential μ is determined by the constraint that the total number of particles in the system is N :

$$N = N_0 + \sum_{\varepsilon \neq \varepsilon_0} N_\varepsilon \rightarrow \mu(N, T) \quad (5)$$

It was recognized by Einstein that the occupation number N_0 of the lowest energy level ε_0 must be treated in a special way in order to avoid divergence of the sum in Eq. 5. It is therefore separated from the rest of the sum. We see from Eq. 4 that $\mu \leq \varepsilon_0$ because the occupation number must be positive.

At room temperature all real gases behave classically, and one can neglect 1 in the BE distribution (Eq. 4). For a rigid 3D box of radius r_0 one can show [3] that:

$$N_\varepsilon \leq N_0 = \left(\frac{\Lambda}{r_0}\right)^3 N \ll 1 \quad (6)$$

which means that all states are about equally and *microscopically* populated.

It is certainly not surprising that at $T = 0$ all particles are in the state of lowest energy. The striking feature of the BE distribution (Eq. 4) is the possibility of a *macroscopic* occupation (of the order of the total particle number N) of the ground state also at finite temperature. Consider what happens to a system of N bosons held at constant volume when we decrease the temperature. To maintain the normalization condition (Eq. 5) the chemical potential μ must adjust by increasing towards the ground state energy $\mu \rightarrow \varepsilon_0$. Below some critical temperature T_c the number of particles in all states except the lowest one can reach the value of N only if $\mu = \varepsilon_0$ and then the chemical potential μ no longer depends on the temperature. [At this point we can draw a clear analogy: For constant μ the BE distribution Eq. 4 coincides with Planck's law describing black-body radiation ($\mu = 0$). The Stefan-Boltzmann law for the total radiation energy density scales as T^4 , and we can easily estimate the number of photons from $N - N_0 \propto E/\hbar\omega \propto E\lambda$, where typical wavelengths are scaling as $\lambda \propto 1/T$ according to Wien's displacement law. The final result, $N - N_0 \propto T^3$,

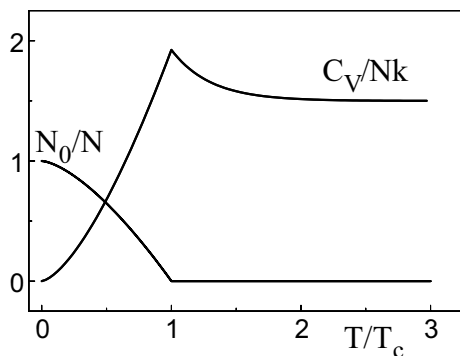


Fig. 1. Important thermodynamic properties of an ideal Bose gas in a large 3D box: fractional number of atoms in the normal and the condensed state (N_0/N) and specific heat (C_V/Nk) as a function of temperature

describes a special but very important case: the occupation of the normal phase (particles with nonzero momentum) of bosonic atoms in a 3D harmonic potential which has a density of states identical to the photon gas (see Eq. 7). Of course, for a photon gas $N_0 = 0$.]

Further cooling further decreases the occupation of all excited states, and all excess particles must go into N_0 . Thus for $T < T_c$ the population of the ground state with zero momentum becomes macroscopic. This is called “condensed phase” while the remaining fraction is called “normal phase.” In a homogeneous system, i.e. in a box with infinite walls, the condensed fraction occupies the same volume as the normal fraction – hence one speaks of “condensation in momentum or k -space.”

This resembles the behavior of a saturated vapor interacting with its solid phase. [It might seem more obvious to compare the quantum phase transition to a vapor-liquid interface. For this system, however, no long-range order is established at the transition point, as is, in contrast, the case for a crystal or a Bose condensate. This situation is also manifested by the existence of a critical point which shows that a liquid and a vapor have the same type of symmetry.] Discontinuous behavior of thermodynamic properties shown in Fig. 1 is also typical of phase transitions. However, in contrast to usual phase transitions caused by intermolecular interactions, Bose condensation is a consequence of the wave function symmetry alone.

Experimental Efforts

It is easy to estimate from Eq. 1 that for air molecules ($M = 28$) and normal density ($N/V = 10^{19} \text{ cm}^{-3}$) the BEC condition is met at $T_c \simeq 40$

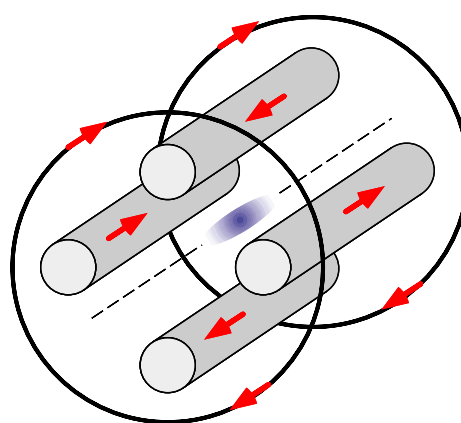


Fig. 2. Magnetic trap for paramagnetic atoms (Ioffe-Pritchard trap). Arrows, direction of the current generating the magnetic field. The magnetic field is designed to create a field minimum in the *central region*. A gas of paramagnetic atoms with magnetic moments antiparallel to the magnetic field lines is confined near the axis of the trap. Because magnetic dipole forces are weak, only slow atoms can be trapped (typically $< 10 \text{ mK}$)

mK. At such cryogenic temperatures, however, air and all other conventional substances have long undergone one or another type of structural phase transition due to intermolecular forces, resulting in a solid phase. Only helium remains liquid down to the thermodynamic zero point and shows unusual “superfluid” behavior below the “lambda point” at 2.17 K. Due to strong interactions, however, its properties deviate widely from predictions for a pure Bose condensate.

BEC was indeed considered an unphysical although highly interesting theoretical concept [3] until experiments were designed to produce quantum degeneracy unobstructed by strong interparticle interactions. One such procedure is to use a dilute spin polarized gas of very cold neutral atoms which are subject to weak interatomic van der Waals interactions only. Paramagnetic atoms can be trapped in suitable magnetic fields, for instance, in the so-called Ioffe-Pritchard trap, shown schematically in Fig. 2. Therefore hydrogen or alkali atoms confined in a magnetic trap had long been predicted [4] to form potentially a Bose condensate. During the 1980s, laser cooling (see e.g., [5]) was turned into an extremely useful tool of experimental atomic physics, and it was applied to atomic gases confined in a suitable trap. Unexpectedly low temperatures in the μK range were observed and opened the route to dramatically increased phase space densities $n\Lambda^3$ (Fig. 3) within sight of the quantum degeneracy borderline. Note that the high phase space density does not coincide with very high particle density of such an ultracold gas in an atom trap. The latter is of order 10^{12} cm^{-3} , which does not exceed the particle density of a good

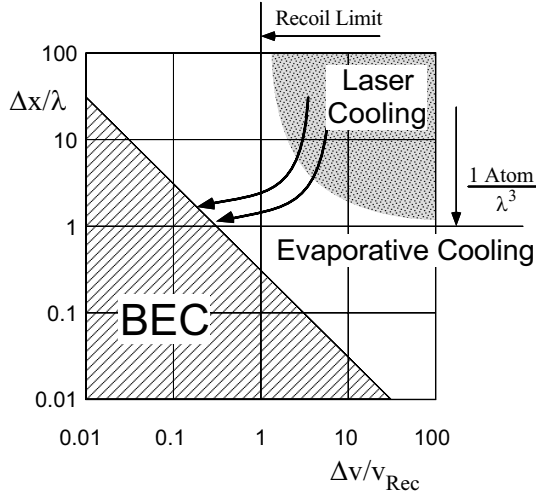


Fig. 3. Phase space accessible by conventional laser cooling techniques and phase space volume of BEC (qualitatively). Spatial coordinates (Δx) are normalized to the cooling laser wavelength (λ), and momentum coordinates ($v = p/m$) to the recoil velocity $v_{\text{rec}} = h/\lambda m$, i.e., the velocity change caused by a single recoil at photon emission or absorption. With laser cooling density remains always less than 1 atom/ λ^3 , and the recoil velocity sets a practical lower limit to the temperature. This diagram is universally applicable to all atoms prepared by laser cooling before evaporative cooling takes the sample to the quantum condensed phase. Note that the entire shaded “BEC” area contains a single unit cell ($= h$) of phase space only

vacuum chamber, corresponding to $\simeq 10^{-5}$ mbar pressure at room temperature.

With slow laser-cooled atoms it was learned to store very cold samples of alkalis for minutes or even hours in magnetic traps, but in spite of large experimental efforts the critical density according to Eq. 3 was not achieved. The presence of laser light set a lower limit to the temperature through heating processes caused by spontaneous emission. At this “recoil limit” the de Broglie wavelength equals the cooling laser wavelength, $\Lambda \approx \lambda$. The limitation of particle densities is caused by multiple scattering of photons (Fig. 3) at the optical density limit $n \approx \lambda^{-3}$.

The most decisive breakthrough was achieved by three groups of experimenters in the United States when they applied the evaporative cooling technique (developed for cooling hydrogen gas [6], which is technically inaccessible to laser cooling) to samples of laser-cooled alkali atoms. Although evaporative cooling is a well-known phenomenon, details of its implementation are indeed crucial, since it is associated with a loss of particles: a Bose condensate can be formed only if the increase in phase space density occurs at a rate faster than the loss rate in particle density [7]. After 3 years of successful operation this method is now well established.

The first and much publicized step across the borderline to a truly degenerate quantum gas of neutral atoms was taken in 1995 by Cornell and coworkers at JILA, Boulder [8], with a gas of spin-polarized rubidium atoms. In the first experiments samples of up to 10^4 atoms were analyzed by 2D-image absorption images (or its shadow) when they were released from the trap (Fig. 4). The condensation was identified through a sudden appearance of a central component of very high optical – and hence particle – density corresponding to a very narrow momentum distribution. It rapidly became possible to carry out measurements of thermodynamical properties of the condensed sample. Excellent agreement with theoretical predictions for the ground state occupation N_0 which in a 3D harmonic potential evolves according to (see “Elementary Predictions”):

$$N_0 = N \left(1 - \left(\frac{T}{T_c} \right)^3 \right) \quad (7)$$

was, for instance, obtained by a measurement of the occupation number in the JILA group [9] (Fig. 5). When the attractive borderline to the quantum degenerate regime was later also crossed by Ketterle and his group at MIT [10] with a sodium sample, dramatic technical advances were soon obtained in the preparation of the condensate (now up to 10^7 atoms in only 30 s) and using a nondestructive dark-field imaging method [36]. It was this breakthrough which opened the route to the observation of condensate interference which is described below.

A third experiment was carried out at the same time by the group of Hulet at Rice University with a sample of lithium atoms [12, 13]. Lithium is interesting since it provides both a bosonic and fermionic isotope for comparative studies. Furthermore, bosonic ^7Li atoms attract each other, and hence the formation of a condensate is completely suppressed in a homogeneous system, i.e., in a large box. A trapping potential can exert a stabilizing influence, however, by confinement of the atoms. Increased zero-point kinetic energies can compensate atomic attraction up to an atomic density depending on the parameters of the potential. A condensate of some 1000 atoms was indeed observed, in fair agreement with theoretical predictions.

Questions in BEC

Einstein’s initial discovery assumed an ideal quantum gas of noninteracting particles in a homogeneous system of infinite extension. In theoretical in-

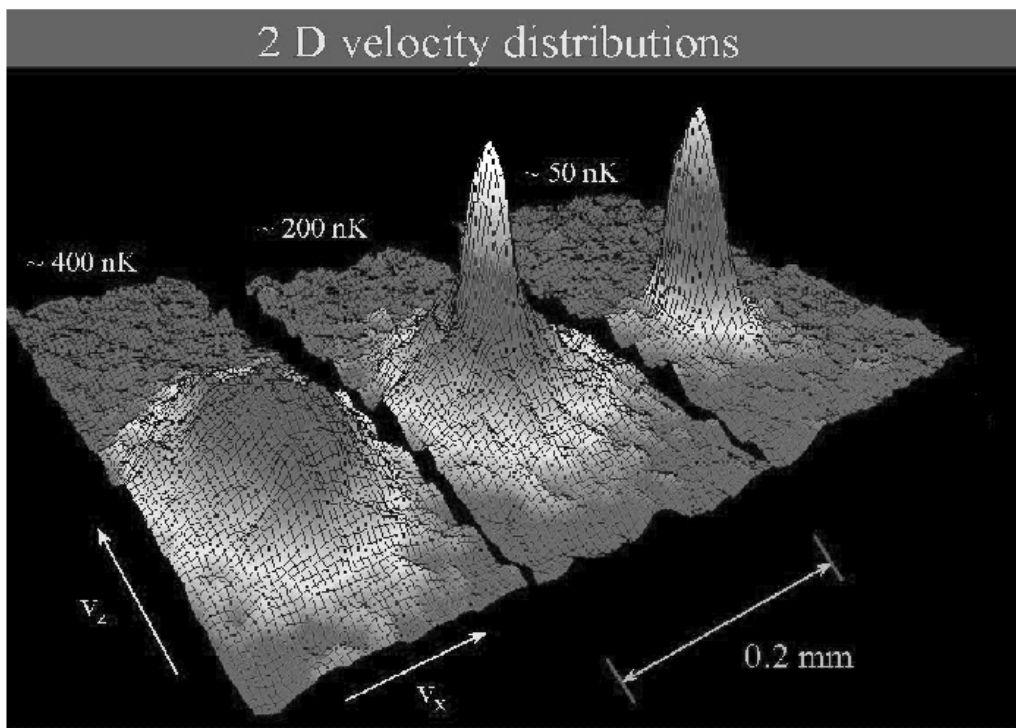


Fig. 4. BEC in a gas of rubidium atoms was first identified by an extremely high optical density in the center of a cooled cloud of atoms. The 2D shadow images were taken 60 ms after the magnetic trap had been switched off, and the cloud had been allowed to expand ballistically. Therefore the image represents the 2D velocity distribution of atom. *From left to right*, the three images were taken just before (thermal Gaussian-like distribution) and just after the appearance of the condensate (two-component cloud with a sharp increase in the peak density), and after further evaporation had nearly left a pure condensate. The condensate fraction is elliptical, indicative that it is highly nonthermal. The temperature can be determined from the noncondensed fraction of atoms (Courtesy E. Cornell [8])

vestigations it was realized early on that a Bose condensate of weakly interacting particles is decidedly more interesting than the ideal gas case. The reason is that noninteracting particles “do not notice each other” – i.e., they cannot have any collective excitations. Theoretical work confirmed that “real” BEC can show surprisingly rich and subtle behavior depending on the details of the considered systems. Atomic condensates may provide a new testing ground for more profound questions concerning the many body quantum nature of a Bose condensate. Below we illustrate several interesting aspects of BEC.

Dimensions. In 1967 Hohenberg demonstrated that BEC can occur only in 3D [14]; this is now known as the Hohenberg–Mermin–Wagner theorem [15, 16]. Why does the intuitively clear picture of overlapping de Broglie wavelengths which is successful in 3D fail in two or one dimension? Furthermore, the impossibility of BEC in 2D and 1D turned out to be valid only for homogeneous systems, that is for systems confined by rigid boundaries. This was first pointed out by Widom [17] who showed that BEC

occurs in a 1D gas in the presence of a gravitational field.

BEC in a Potential. In all experiments described above atoms are confined by a spatially varying potential. In this case the coupling between energy and space fundamentally alters the nature of BEC. In general, a trapping potential supports BEC [18]: as the mean energy decreases, the effective volume available to the system also decreases enhancing the growth of density. For example, in a power-law potential BEC is always possible in two dimensions, while 1D systems were predicted to display BEC in traps that are more confining than parabolic [19]. Formally it is sufficient to evaluate the density of states to resolve the quest for quantum degeneracy in a potential.

Finite Numbers of Particles. The usual theory of BEC assumes the thermodynamic limit of an infinite system. An investigation of an ideal gas with a *finite* number of particles [20] has shown that the transition temperature in a 3D harmonic potential is lower than in the thermodynamic limit, as one would expect. Surprisingly, however, BEC in a 1D harmonic potential can also occur if N is finite.

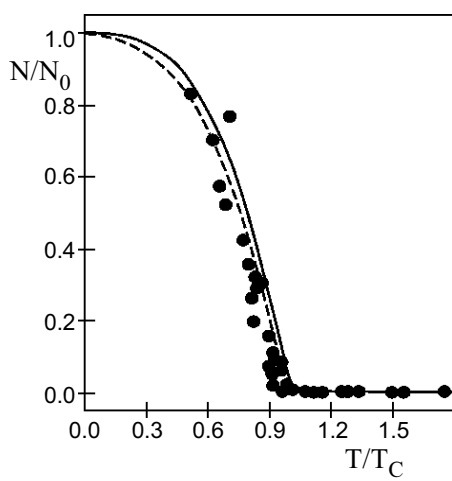


Fig. 5. Fractional occupation number N_0/N of the ground state in a Bose condensate as a function of temperature. The scale temperature $T_c(N)$ is the predicted critical temperature for an ideal Bose gas in a harmonic potential. *Solid line*, expected occupation number for an infinite number of particles; *dashed curve*, takes a finite number of atoms into account (see Eq. 7). (Courtesy E. Cornell [9])

Particle interactions. In a real gas interparticle interactions are extremely important and can totally change the behavior of the system, especially in the low-dimensional case. They are responsible for the finite compressibility of the condensate and therefore for the existence of sound modes at long wavelengths instead of free particle excitations. Obviously the interactions are also very important for the onset of condensation and for the build-up of coherence in matter waves, which is a field of active research.

Generalized BEC Condition for Potentials and Lower Dimensions

The conditions for a macroscopic population of the ground state can be summarized by a transparent formula which is derived from an analysis of the phase space volume available to the system (see “Appendix”). In d dimensions we find for a system with N particles and a de Broglie wavelength Λ according to Eq. 2 the simple relationship which is in comforting agreement with our physical intuition:

$$\Lambda^d \frac{N}{V^*} \approx 1 \quad (8)$$

and in direct analogy with Eq. 3. The primary focus of this formula is the introduction of an effective volume $V^* \approx r^d$ which for an isotropic power-law potential $U(r) \propto r^n$ is determined from the condition $kT \approx U(r)$. Let us demonstrate how well this formula works with two examples.

BEC in Trapping Potential. The ground-state population fraction for $T < T_c$ is given by (see “Appendix”):

$$\frac{N_0}{N} = 1 - (T/T_c)^\eta \quad (9)$$

with $\eta = d/2 + d/n$, reproducing the original prediction by Einstein $\eta = 3/2$ for a homogeneous system ($d = 3, n = \infty$) and (Eq. 7) $\eta = 3$ for a 3D-harmonic trap ($n = 2$) as in current experiments

Two-Dimensional Systems. When in a homogeneous 2D system ($d = 2, n = \infty$) the volume V^* is restricted to the surface area S we immediately obtain from Eq. 8 a critical temperature:

$$T_c = \frac{\pi \hbar^2}{2km} \frac{N}{S} \quad (10)$$

This result agrees perfectly with the transition temperature deduced for a so-called quasi-condensate with short-range correlations (or Kosterlitz-Thouless phase [21]). Note, however, that our argument allows an estimate only for the onset of quantum degeneracy. The stability of such a “condensate” must be determined from a more elaborate analysis.

Interactions and Sound in the Condensate

Although the occurrence of a phase transition on pure quantum mechanical grounds has captivated the minds of physicists ever since its discovery, Bose–Einstein condensates would be rather boring objects if it weren’t for the interactions within this appealing state of matter. In a gas of noninteracting Bose particles the energy structure of the noncondensed sample is preserved, and the only effect of excitations is to remove individual particles from the condensed state. A quantum condensate of interacting particles, however, can react collectively to an external disturbance exhibiting low lying and novel excitations within the condensed state. For instance, helium in its quantum fluid state exhibits unusual phenomena related to such disturbances which are usually called “sound.”

It is indeed due only to the interaction of the condensed particles, or the finite compressibility, that disturbances of, for instance, the density propagate in a nontrivial manner.

Mean-Field Energy

In a gas of noninteracting particles residual velocities are determined by the zero-point kinetic energies

in the trapping potential only. In contrast, the high density of the condensate causes the average intermolecular potential energy in the condensate to be much greater than kinetic energies. Once the confining potential is switched off, the corresponding internal pressure is released and dominates the expansion.

At very low relative velocities (“cold collisions” [22]) rubidium and sodium atoms repel each other. Since the interaction is of short range, it is justified to describe the atom-atom interaction energy by a simplified pseudopotential:

$$U(\mathbf{r}) = \frac{4\pi\hbar^2 a}{m} \delta(\mathbf{r}) \quad (11)$$

where the δ function denotes the quasipointlike interaction. The relevant “s wave scattering” length a is positive for ^{87}Rb ($a = 60 - 100 \text{ \AA}$ [23]) and ^{23}Na ($a \simeq 27 \text{ \AA}$ [24]) but negative for ^7Li ($a = -15 \text{ \AA}$ [25]). The condensate is called “weakly interacting” if the particle density n satisfies condition:

$$na^3 \ll 1 \quad (12)$$

as is the case for the existing atomic Bose condensates. In other words, the scattering length a remains very small compared to interatomic separations.

For an individual atom the contribution of all other atoms in a condensate is proportional to the local density $n(\mathbf{r})$ and gives rise to the mean field energy by:

$$U_{\text{MF}}(\mathbf{r}) = \frac{4\pi\hbar^2 a}{m} n(\mathbf{r}) \quad (13)$$

and therefore proportional to the density N/V . An atomic Bose condensate is formed in a harmonic potential which allows the condensate to expand with N and weakens the N dependence of U_{MF} . For $T \rightarrow 0$ the meanfield energy can also be identified with the chemical potential, $\mu \rightarrow U_{\text{MF}}$.

The mean field energy becomes clearly negative for attractive interaction or negative scattering length a , which is the case for ^7Li and prevents BEC from occurring in a large homogeneous system. It can, however, be compensated by the zero-point energy $\hbar^2/m\ell_0^2$ if the atoms are confined to volume of radius ℓ_0 . This limits the maximum number of atoms in the metastable condensate to [26]

$$N_0(\text{max}) \simeq \frac{\ell_0}{|a|} \quad (14)$$

The BEC criterion used above (macroscopic occupation of the lowest single particle energy level Eq.

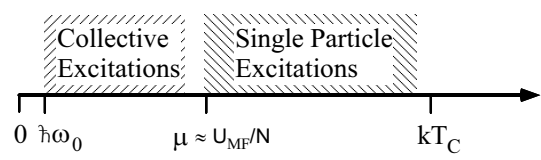


Fig. 6. Energy scales of a weakly interacting BEC. For a single particle excitation, or removal of an atom from the condensed state an energy above the gap is required. The lowest excitation energies (or oscillation frequencies) below the energy gap always correspond to intrinsic many body phenomena, or collective excitations

8) is meaningful for noninteracting particles only. In order to account for interactions we introduce a wavefunction which relates each atom in the condensate to the total particle density $n(\mathbf{r})$ through:

$$n(\mathbf{r}, t) = N |\psi(\mathbf{r}, t)|^2 \quad (15)$$

The Schrödinger equation can then be constructed from the the harmonic oscillator potential $V(\mathbf{r}) = m\omega_0^2 \mathbf{r}^2/2$ and an effective single atom potential caused by the meanfield energy per atom, $U_{\text{MF}} \cdot n(\mathbf{r}) = 4\pi\hbar^2 a/m \cdot |\psi(\mathbf{r})|^2$:

$$i\hbar \frac{\partial}{\partial t} \psi(\mathbf{r}) = \left(-\frac{\hbar^2}{2m} \nabla^2 + V(\mathbf{r}) + \frac{4\pi\hbar^2 a}{m} |\psi(\mathbf{r})|^2 \right) \psi(\mathbf{r}) \quad (16)$$

Within the framework of BEC this nonlinear Schrödinger equation is better known as the Gross–Pitaevski equation [27, 28, 29]. An analysis of the minimum energy state shows that in spite of the volume increase in the condensate, caused by increasing intermolecular energy the chemical potential μ in a harmonic trap still grows as $N^{2/5}$ resulting in a mean field energy much larger than but also proportional to the oscillator energy $\hbar\omega_0$ [30]. In the so-called Thomas-Fermi approximation kinetic energy terms in the Gross-Pitaevski equation (Eq. 16) are completely negelected.

In Fig. 6 we summarize the energy scales relevant for a weakly interacting Bose condensate. The average mean field energy $U_{\text{MF}} = 4\pi\hbar^2 a/m \sim \mu$ of Eq. 13 is also an estimate of the energy required to transfer a single atom from the condensed to the normal state [3]. This “energy gap” constitutes a threshold for single particle effects.

Vibrations of Atomic Condensates

We concentrate on the case where the mean free path of a condensate atom is much shorter than the extension of the condensate, establishing a local density equilibrium. Furthermore, at $T/T_c \ll 1$ the normal

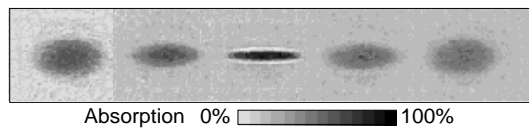


Fig. 7. Quadrupolar shape oscillation of a cigar like condensate. The oscillation period (20–50 ms) agrees well with theoretical predictions from the mean field model. (Courtesy W. Ketterle [11])

phase is virtually absent, it can be neglected, and a pure condensate oscillation is expected.

In an experiment the trapped condensates may be excited by (periodically) changing the magnetic trapping fields or by exerting additional forces through optical forces derived from a laser beam focused into the condensate. Oscillations with frequencies in the 10–500-Hz domain have been observed [32, 11].

It is possible to excite collective mechanical excitations of the condensed state which may be compared to the normal mode oscillations observed with standing sound waves in a liquid droplet confined to a harmonic potential. The simplest motion is the center of mass oscillation at the trapping potential frequency. This is called “dipole mode” and is in fact the lowest frequency excitation – for small displacements it does not change shape and hence the mean field energy of the object. Shape oscillations of quadrupolar character have also been observed [32, 11, 33]. An example of the strobed shape variation is shown in Fig. 7.

A theoretical analysis based on a linearized approximation of the Gross-Pitaevski (Eq. 16) gives an analytic solution in the hydrodynamic limit [30] and excellent numerical agreement with experimental observations for the lower density case [33, 34]. Meanwhile, not only standing but also propagating sound waves have been observed [35], lending still more support to the mean field approach. Note, however, that the modification of oscillation frequencies is a result of hydrodynamic flow and interactions only and does not prove the quantum wave character of the condensed sample. For an experimental investigation of this phenomenon it is necessary to study interferences, or correlations of particle densities.

Matter Waves

When “immaterial” optical waves are discussed we are not surprised when their nature becomes manifest through the occurrence of interference. When it comes to matter waves, however, the concept of interference still seems to be at odds with our imagination of particles.

Indeed, the well-known quantum-mechanical analogy between light and matter, first recognized by

de Broglie and manifested in diffraction experiments with electrons, has very severe limitations. For example, there can be no classical field theory for electrons [36]. To see this, we can consider a scalar field

$$\psi = Ae^{i\phi} \quad (17)$$

with a phase ϕ and an amplitude A normalized on such a scale that $A^2 = N$ is the number of quanta per field mode. Then the uncertainty relation is

$$\delta N \cdot \delta\phi \geq 1 \quad (18)$$

If we want to treat the field as a classical quantity the uncertainty in the phase should be small compared to unity, and the uncertainty in N should be small compared to N itself. According to Eq. 18, however, this requires that $N \gg 1$. If we recall that N is the number of quanta per mode, we see that a classical field description is forbidden for fermions by the Pauli principle. This difficulty does not apply to a boson field and one can verify that a laser beam is usually intense enough (the photon number is macroscopic!) to allow amplitude and phase to be known with good precision [37]. The uncertainty of the particle number in the coherent state poses no problems for photons. Application of this concept to material particles such as bosonic atoms left a rather uncomfortable feeling, however.

Recent experiments carried out at MIT demonstrate unambiguously that coherent matter waves do exist at a macroscopic scale. Let us examine experiments which have begun to explore the true quantum nature of an atomic Bose condensate, or the existence of an amplitude and a macroscopic phase according to Eq. 17.

Interfering Bose Condensates

Dramatic experimental progress in both preparing and observing Bose condensates has enabled the MIT group to record an image of two interfering condensates of Na atoms [38]. For this experiment the cigar shaped-magnetic potential was cut into two halves by means of a focused far-off resonant laser beam which allowed synchronous preparation of two neighboring but independent condensates. The samples were then released from the trap and interfered on expansion. They overlap horizontally, and interference fringes with a spacing of about $15 \mu\text{m}$, and a contrast of 20–40% are clearly visible in Fig. 8. Note that the image is derived from a single event of condensate ejection since the relative phase of the condensates varies randomly from shot to shot. This experiment provides the first direct image of

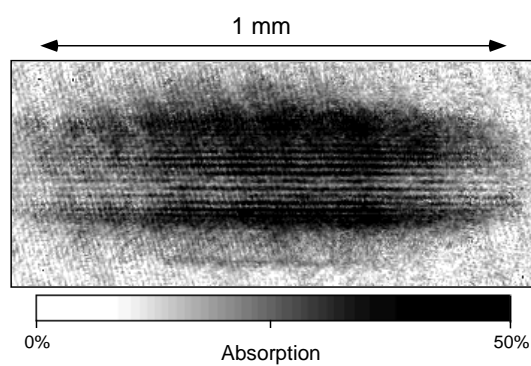


Fig. 8. Interference pattern of two Bose condensates. The fringes are due to periodic density variations of the interfering condensates. Since the pattern has a random global phase in each event, it must be recorded in a single shot. This experiment demonstrates interference of matter waves beyond single particle self interference. (Courtesy W. Ketterle [38])

matter waves interference. Earlier experiments always relied on self-interference of individual particles transmitted through an appropriate matter wave beam splitter and recombined – a mind-boggling phenomenon by itself, but clearly on the microscopic scale!

The observed interference wavelength can be understood in terms of relative atomic motion. When the two samples are released from two points separated by a distance d , they freely fall and expand transversely at the same time. After a time t has elapsed condensate portions moving at $v = d/t$ overlap and have a relative de Broglie wavelength $\Lambda = ht/md$. The interference pattern observed agrees well with this rough estimate and also with more detailed theoretical analysis [41].

A Coherent Matter Wave Generator

A first step towards generation of propagating coherent matter waves was also taken by the MIT group. Using radiofrequency excitation it is possible to extract smaller portions of the condensate, as shown in the strobed image of Fig. 9.

The question of whether two coherent light fields emanating from two independent laser sources can interfere at all was debated very intensely shortly after the laser was invented – and rapidly settled as well [40]. The observation of interference from two independent atomic Bose condensates has already prompted the term “atom laser” in analogy to a conventional laser, even though in contrast to the optical laser robust and compact instruments are not yet available and this designation is still under debate [41]:

An atom laser is a device which generates an intense coherent beam of atoms through

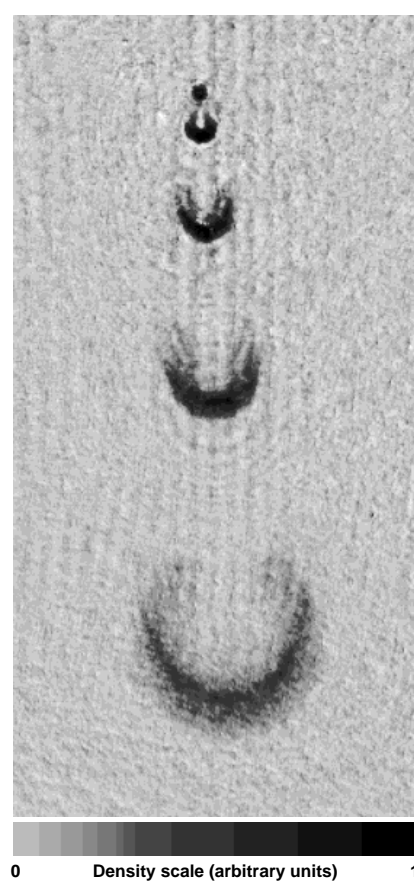


Fig. 9. Pulses of coherent matter in free fall. The samples have been extracted periodically from the stored condensate (top) by radiofrequency excitation. Their coherence is demonstrated by the experiment presented in Fig. 8. (Courtesy W. Ketterle).

a stimulated process. It does for atoms what an optical laser does for light. The atom laser emits coherent matter waves whereas the optical laser emits coherent electromagnetic waves. Coherence means, for instance, that atom laser beams can interfere with each other... .

Beyond the Pedestrian’s Approach to BEC

In the preceding sections we analyze the phase space volume available for a quantum system depending on dimension or potential shape, yielding estimates for the onset of quantum degeneracy in a Bose gas of atoms. Intuitive guidance for wave mechanical effects is introduced by an analogy with classical waves which are described by an amplitude and by a phase. There is no consideration above of the stability of such a system, however, which is determined not only by the total energy of a system but also by

the entropy S . This competition is usually described by the so-called Helmholtz free energy F :

$$F = E - TS \quad (19)$$

which is minimized in thermal equilibrium. We do not analyze the entropy S of a Bose condensate in detail but rather give a direct way to calculate the free energy which is an example of a *thermodynamic potential*.

It is the purpose of this section to introduce the reader to these important but more subtle aspects of BEC, mostly on the basis of analogies. Let us try the unspeakable and describe some of the abstract concepts fascinating real theorists.

Fundamental Concepts of Many-Body Quantum Physics

Formally the transition from classical to quantum statistical mechanics involves replacement of classical quantities such as the energy E by their operator analogue, in this case the Hamiltonian \hat{H} . The state of a microscopic system is then given by the expected value of the operator for a quantum state characterized by a wavefunction ψ . For instance, the energy of a quantum state is calculated from:

$$E = \int \psi^* \hat{H} \psi \quad (20)$$

A thermodynamic system consists of an enormous number of particles. It is no longer the state of every individual particle that we are interested in. It is rather the knowledge of quantities such as temperature or pressure of the sample which can be analyzed by statistical methods. For this purpose we use the density matrix $\hat{\rho} = \exp(-\beta\hat{H})/Z$, which describes the occupation probability of individual quantum states, and where $\beta = 1/k_B T$ is the inverse temperature. The expectation value of the operator:

$$Z = \text{Trace} \{ \exp(-\beta\hat{H}) \} \quad (21)$$

is called partition function (in German *Zustandsumme*), it is a sum running over all quantum states and assures the correct normalization of the density matrix. The partition function is intimately related to the free energy (Eq. 19) of a physical system:

$$F = -k_B T \ln(Z) \quad (22)$$

Once the partition function is known, all thermodynamic parameters can be derived from it.

Time evolution of a microscopic quantum state is described by the Schrödinger equation, and there exists

a close formal analogy between the equation describing the time evolution of the density matrix:

$$i\hbar \frac{\partial}{\partial t} \psi = \hat{H} \psi \quad \rightarrow \quad \hbar \frac{\partial}{\partial \tau} \hat{\rho} = -H \hat{\rho} \quad (23)$$

The only formal difference is that the time in the Schrödinger equation must be replaced by an imaginary “time,” $t \rightarrow -i\tau$, which has the unit of an inverse energy and runs from 0 to β .

A very elegant approach to analyzing the evolution of a quantum system is the method of path integrals. The transition amplitude of the microscopic system from an initial point (x_i, t_i) to a final point (x_f, t_f) can be expressed by a path integral over all paths leading from x_i to x_f :

$$U(x_f t_f, x_i t_i) = \langle x_f | e^{\frac{i}{\hbar} H(t_f - t_i)} | x_i \rangle = \int_i^f D[x(t)] e^{\frac{i}{\hbar} S[x(t)]} \quad (24)$$

Here $D[x(t)]$ is a generalized integration variable demanding an integral over all the possible paths that a particle can take. The action for a given path $S[x(t)]$ is defined by:

$$S = \int_{t_i}^{t_f} dt L[x(t)] \quad (25)$$

where L is the Lagrangian of the system, with contributions of the kinetic energy and of the relevant potentials:

$$L = \frac{m}{2} \left(\frac{dx}{dt} \right)^2 - V(x) \quad (26)$$

For example, the partition function, Z , for a *single particle* can be viewed as the trace of the time evolution operator in imaginary time if we write the partition function (Eq. 21) as a trace over the position eigenstates:

$$Z = \text{Trace}(e^{-\beta\hat{H}}) = \int dx \langle x | e^{-\beta\hat{H}} | x \rangle \quad (27)$$

To carry out the analogy we express the transition amplitude again as a path integral over all possible trajectories of the system:

$$U(x_f \tau_f = \beta, x_i \tau_i = 0) = \langle x_f | e^{\frac{1}{\hbar} H(\tau_f - \tau_i)} | x_i \rangle = \int_i^f D[x(\tau)] e^{-\frac{1}{\hbar} S[x(\tau)]} \quad (28)$$

In analogy to (Eqs. 25 and 26), the microscopic action S and the Lagrangian are now given by:

$$S = \int_{\tau_i=0}^{\tau_f=\beta} d\tau L[x(\tau)] \quad (29)$$

and

$$L = \frac{m}{2} \left(\frac{dx}{d\tau} \right)^2 + V(x) \quad (30)$$

We can now implement this method for many-body systems by replacing the microscopic Lagrangian (Eq. 30) by the Lagrangian of the macroscopic system. In the path integral we must sum over all possible paths of the entire physical system. This task may be simplified by the use of an appropriate representation.

Coherent States and Expectation Values

The coordinate representation of the wave function turns out to be an awkward description for the many-body system. Fortunately, there exists a more useful basis, the basis of coherent states which is illustrated in more detail in the next section. A coherent state, $|\phi\rangle$, can be defined as the eigenstate of the annihilation operator for particle fields, $\hat{\psi}$:

$$\hat{\psi} |\phi\rangle = \psi |\phi\rangle \quad (31)$$

The basis of coherent states, $|\phi\rangle$, is characterized by their eigenvalues, ψ , which for bosons are just complex numbers. For the evaluation of expectation values of many-body systems also “adjoint” coherent states $|\bar{\phi}\rangle$ with eigenvalue $\bar{\psi}$ are used instead of the complex conjugate of the wave function used for single particle systems. The coherent state representation of the path integral is obtained by inserting the basis of the coherent states at every step into the time evolution.

The final form of the partition function is then:

$$Z = \int D[\bar{\psi}, \psi] e^{-S_{\text{mac}}(\bar{\psi}, \psi)/\hbar} \quad (32)$$

where the macroscopic action S_{mac} is given in terms of the coherent states ψ and $\bar{\psi}$ by:

$$S_{\text{mac}}(\bar{\psi}, \psi) = \int_0^\beta d\tau L_{\text{mac}}(\bar{\psi}, \psi) \quad (33)$$

The advantage of this approach is that we can in fact evaluate any thermal expectation of a physical observable \hat{A} value from a path integral:

$$\langle \hat{A} \rangle = \int D[\bar{\psi}, \psi] e^{-S_{\text{mac}}(\bar{\psi}, \psi)/\hbar} \hat{A}(\bar{\psi}, \psi) \quad (34)$$

Properties of Coherent States

Before we proceed to describe properties of a Bose condensate let us illustrate properties of the macroscopic wave functions ($\psi, \bar{\psi}$) introduced in the previous paragraph. Matter is described in terms of quantum fields which are associated with field operators, $\hat{\psi}(r), \hat{\psi}^\dagger(r')$. The particle density operator is $\hat{n}(r) = \hat{\psi}^\dagger(r)\hat{\psi}(r)$, similar to the relationship of the intensity and the amplitude of a light field. Extending the analogy to light field interference we may also define a (first order) correlation function through $\rho(r, r') = \langle \hat{\psi}^\dagger(r)\hat{\psi}(r') \rangle$ which reproduces the density for $r' = r$. Note that this quantity is measurable for a single sample only if it is split and recombined, for instance, by two beam interference in a Michelson type interferometer. Alternatively, two independently prepared samples may be brought into interference, and exactly this was demonstrated in the matter wave interference experiment at MIT [38]. A normal fluid is disordered at large distances, and hence there is no correlation except for the immediate vicinity of particles (at $|r - r'| \rightarrow 0$). In a quantum liquid such as superfluid helium, however, correlations do exist at large separations, prompting Penrose and Onsager [42] to introduce the concept of “off-diagonal” long range order where the density correlation function factorizes in a special way:

$$\begin{aligned} \text{for } |r - r'| \rightarrow \infty : \\ \text{normal fl. } \langle \hat{\psi}^\dagger(r)\hat{\psi}(r') \rangle &\rightarrow 0 \\ \text{quantum fl. } \langle \hat{\psi}^\dagger(r)\hat{\psi}(r') \rangle &= \langle \hat{\psi}^\dagger(r) \rangle \langle \hat{\psi}(r') \rangle \neq 0 \end{aligned} \quad (35)$$

In particular it does not vanish even at large separations, and it is this criterion which is now taken as the most satisfactory definition of a macroscopic quantum state such as a Bose condensate [43]. Coherent states are then an obvious choice for a formal description of such systems.

The coherent state representation of the path integral (Eqs. 32, 34) is particularly suited for describing the “off-diagonal long range order.” Coherent state wave functions are also widely used to describe properties of a laser light field [37].

The order is characterized by a complex order parameter, ψ , which has amplitude and phase. The phase is a macroscopic dynamic variable of the system and possesses real physical meaning. The number operator, \hat{N} , and the phase operator, $\hat{\phi}$, are conjugate variables, with expectation values obeying the uncertainty relation of Eq. 18, as one can easily derive from the definition of the coherent states. It is furthermore possible to reconstruct a state with a fixed number of particles, N , from the coherent state of

the condensate $\bar{\psi}_{cond} = \sqrt{\rho}e^{-i\phi}$ by averaging over the phase of the wave function:

$$\int_0^{2\pi} \frac{d\phi}{2\pi} e^{-i\phi N} |\psi_{cond}\rangle = \sqrt{\frac{\rho^N}{N}} |N\rangle \quad (36)$$

Mean-Field Approximation

Our focus is directed towards an imperfect Bose gas with coupling constant $g = 4\pi\hbar a^2/m$, in a potential $U(\mathbf{r})$, governed by a chemical potential μ , and kinetic energy $\epsilon_p = p^2/2m$. In this case the action S is given by:

$$S = \int_0^\beta d\tau \int d^3r \left\{ \hbar\bar{\psi} \frac{\partial}{\partial\tau} \psi + \frac{\hbar^2}{2m} |\nabla\psi|^2 + (U(\mathbf{r}) - \mu)|\psi|^2 + \frac{g}{2} |\psi|^4 \right\} \quad (37)$$

The important contributions to the partition function, Z , according to Eq. 32 come from configurations where the action, S , is small. The mean-field approximation is obtained by expanding the action S to quadratic order in $\bar{\psi}$ and ψ around such a stationary point. The free energy, F , is then given by:

$$F = -k_B T \ln \left(\int D[\bar{\psi}, \psi] e^{-S(\bar{\psi}, \psi)/\hbar} \right) \approx k_B T S(\bar{\psi}_{MF}, \psi_{MF})/\hbar \quad (38)$$

In Fig. 10 the potential contribution to Eq. 37 corresponding to the free energy in this case is shown as a function of the order parameter ψ :

The stationary point in time and space of the action, S , is determined by a nonlinear Schrödinger equation for the field, ψ , and recovers the stationary case of the Gross-Pitaevski (Eq. 16):

$$-\frac{\hbar^2}{2M} \nabla^2 \psi + (U(\mathbf{r}) - \mu)\psi + g|\psi|^2\psi = 0 \quad (39)$$

There are two solutions to this equation. The first is $\psi = 0$. This is the normal state, no coherent state with finite amplitude $|\psi|$ is occupied. The second has a finite ψ . The mean-field solution, ψ , possesses a well-defined global phase ϕ which is arbitrary but fixed. The original action (Eq. 37) is invariant under a global change of the phase ($\psi \rightarrow \psi e^{i\varphi}$).

The mean-field solution, ψ , picks out a certain direction of the phase angle ϕ , which is called spontaneous symmetry breaking, where in the language of group theory it is $U(1)$ group symmetry of phase transformations, which is violated. The phase of the mean-field, ψ , is coherent over the entire system.

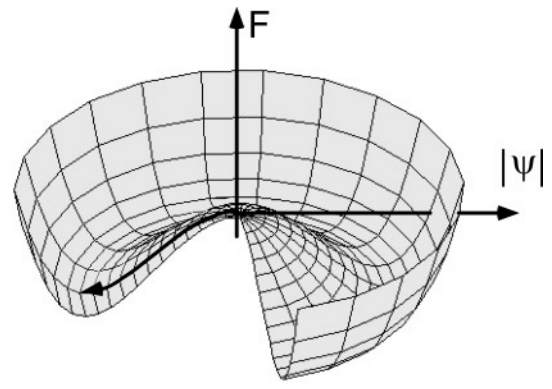


Fig. 10. Thermodynamic potential (free energy) as a function of the order parameter ψ . Note that it corresponds to the potential term in Eq. 37. The lowest energy state has a single selected phase (arrow) which is valid for the entire condensate. This situation has been named “spontaneous symmetry breaking.” Variations in the amplitude are called “longitudinal excitation,” fluctuations of the phase “transverse excitation.” This designation can be traced back to quantum descriptions of ferromagnetism, a phase transitions with analogies to BEC

Fluctuations

In the previous section we discuss the mean-field expectation value for the order parameter. The question is whether the mean-field solution is stable. Since this depends on the spatial dimension of the system, we discuss here a general homogeneous system in d dimensions. The order parameter can be destroyed by thermal or quantum fluctuations. To obtain the contribution of the fluctuations we expand the action S (Eq. 37) to second order in the fields $\bar{\psi}$ and ψ around the saddle point solution $\psi_{MF} = |\psi_{MF}|e^{i\phi}$. Choosing the (arbitrary) phase, $\phi = 0$, the longitudinal, ψ_L , and transverse ψ_T , fluctuations change the mean field to $\psi_{MF} \rightarrow \psi_{MF} + \psi_L + i\psi_T$. The field ψ “moves” in a potential depicted in Fig. 10.

Obviously there exist two kinds of excitations. One corresponds to longitudinal fluctuations, ψ_L , of the order-parameter which have a gap, and another corresponds to a global rotation of the phase, ψ_T , and has no gap in the long-wavelength limit – so-called Goldstone modes. We can see this formally if we examine the the action of the fluctuations:

$$S = \int_0^\beta d\tau \int d^d r \frac{1}{2} \times \left\{ \left(\frac{\partial}{\partial\tau} \psi_L \right)^2 + (\nabla \psi_L)^2 + \Delta^2 \psi_L^2 + \left(\frac{\partial}{\partial\tau} \psi_T \right)^2 + (\nabla \psi_T)^2 \right\} \quad (40)$$

where Δ is the mean-field value of the field ψ and ψ_L , and ψ_T are the coordinates of the longitudinal and transverse fluctuations, respectively. From

Eq. 40 we can read off the dispersion of the longitudinal and transverse mode:

$$\omega_L^2(q) = \Delta^2 + q^2 \quad (41)$$

$$\omega_T^2(q) = q^2 \quad (42)$$

The longitudinal mode corresponds to oscillations in the amplitude of the order parameter. The order parameter is robust since a change in magnitude requires energy which causes a finite energy gap for the longitudinal mode. Excitations of the transverse mode, however, cost very little energy and therefore begin without a gap. In this case the wave number q may be understood as the lengthscale over which the phase of the condensate varies in the sample.

Stability of the Condensate

The mean-field “condensate” is stable if small perturbations due to thermal noise or quantum fluctuations do not significantly change the state of the system. This stability of the system (the amount of “noise”) can be investigated by determining the correlation function of the fluctuations, which are dominated at sufficiently low temperatures by transverse excitations (Eq. 42) without energy gap. Their contribution can be estimated from an analysis of their density of states in q space:

$$\langle \psi_T(\mathbf{r}, \tau) \psi_T(0, 0) \rangle \sim \int (dq)^d \frac{e^{-i\mathbf{q}\mathbf{r}}}{q^2} \quad (43)$$

If this correlation function diverges small external fields – or noise – have a dramatic effect on the phase of the system. For spatial dimensions $d > 2$ the integral always converges at $q = 0$. The Goldstone-modes disorder the system but result in a finite reduction in the order parameter only. In spatial dimensions of $d = 2$ or less the effect of fluctuations is more dramatic. They can disorder the system completely, which is the basic content of the Hohenberg-Mermin-Wagner theorem [14–16].

Another way to understand the existence of a lower critical dimension is to investigate the competition between entropy and energy in the free energy, according to Eq. 46. Let us for this purpose draw on another analogy with ferromagnetism. The minimum energy state of a simple isotropic ferromagnet is characterized by domains which have internally homogeneous magnetization but different orientations. Energy is stored in the walls separating these domains. In analogy, a Bose condensate may consist of domains having constant phase which are separated by domain walls. The energy associated with

twisting the phase locally is parametrized by a phase stiffness, ρ_0 , which has the units of energy per length squared. The energy of such a domain wall scales with the linear dimension of the system L as:

$$E \sim \rho_0 L^{d-2} \quad (44)$$

[The phase varies continuously over the domain wall. This is different from an “Ising” domain-wall where $E \sim \rho_0 L^{d-1}$ as naively expected.] On the other hand, we might place the domain wall anywhere. The number of possible configurations is L^d and therefore the entropy connected with the domain wall is:

$$S \sim d \ln L \quad (45)$$

The free energy of the system with the domain wall is approximated by:

$$F \sim \rho_0 L^{d-2} - T d \ln L \quad (46)$$

For $d > 2$ the first term always dominates the free energy for low enough T , and the ordered state is stable. For $d < 2$ the second term, entropy, dominates and the ordered state is disordered by domain walls. Hohenberg [14] and Mermin and Wagner [15, 16] made these statements more precise and showed that the lower critical dimension for a homogeneous superfluid is 2.

Confined Systems

All experiments to date have been carried out in a 3D potential. According to our estimate, the influence of fluctuations due to the low energy “phase” mode leads to disorder (or entropy) but is not sufficient to destroy phase coherence. Moreover, confinement due to the trapping potential causes even the lowest phase mode excitation to have a finite frequency, ω , the trap frequency, due to space quantization. Therefore BEC is actually easier to achieve in a potential because entropy, which is already dominated by energy, is further suppressed. This is also true in moderately anisotropic traps [44].

However, we can easily imagine experimental situations where the atomic clouds are put into a reduced dimensionality. In strongly anisotropic traps the condensate stability question becomes more interesting again. If for example one spatial extension, say, in the z direction, becomes much larger than the other two, the trap frequencies, ω_z , depend continuously on the “wave number,” q_z . The spectrum has a discrete structure for the perpendicular quantum numbers ($\omega_\perp \ll \omega_z$). If the spectrum of the lowest branch is dense enough (the linear extension

of the cloud in the z direction being very large), the long-range order can be destroyed again due to phase fluctuation [45]. This can be also derived from the observation that the 1D harmonic trap and the 2D homogeneous system have an identical density of states. The 1D system may give experimental access to an extreme system where the scattering length a is greater than the transverse extension of the system. When in this situation the particles of the condensate can no longer pass each other, the spectacular difference of bosons and fermions disappears! This entanglement of dimensionality, potential shape and quantum statistics and many other unanswered questions are now a subject of increasing activity in theory and experiment.

Summary

The novel Bose quantum systems now available experimentally are exerting a strong impact on both atomic and condensed matter physics. On the one hand, we must conclude that there have been no real surprises so far; theoretical predictions have proven well founded. On the other hand, atomic Bose condensates have just begun to open a unique experimental opportunity with unanticipated flexibility in comparison with liquid helium. Magnetic confinement completely isolates the system from any walls leading to a most refined situation where the kinetics of the sample undergoes pure self-evolution; design of the magnetic trap allows extremely anisotropic situations to be achieved, yielding lower than three-dimensionality; evaporative cooling control allows the number of particles to be varied. Furthermore, atomic Bose condensates have allowed us to peek into the possibility of having a coherent matter wave generator at hand – an intellectually and technically highly attractive tool with consequences which cannot be foreseen today. No doubt BEC will shape many physics laboratories in the future, where extended work on condensed matter physics with methods of atomic physics is the next step.

We thank Eric Cornell and Wolfgang Ketterle for providing their figures for this review.

Appendix: Density of States and Quantum Degeneracy

For an atom trap that produces energy-level spacings which are microscopic compared to the mean energy ($kT \gg \varepsilon_{i+1} - \varepsilon_i$), the sum in Eq. 5 can be evaluated by converting it into an integral:

$$N = N_0 + \int_0^\infty N_\varepsilon \rho(\varepsilon) d\varepsilon. \quad (47)$$

[$\varepsilon_{i+1} - \varepsilon_i$ is of the order of the energy of the first excited state which for a power-law potential is given by h^2/mr_0^2 . For example, for a box the validity of the semiclassical approximation is equivalent to the condition $r_0 \gg \Lambda$, and for a harmonic potential to $kT \gg \hbar\omega$.] Here the ground-state energy is taken to be zero. The density of states $\rho(\varepsilon)$ depends on the trapping potential $U(\mathbf{r})$ and the number of degrees of freedom. To visualize the interplay between the dimensionality and the potential shape let us consider a simple example of an ideal Bose gas in an isotropic potential $U(r)$ in d dimensions. Noting that the number of states equals the phase space volume divided by h^d , we calculate the density of states from:

$$\begin{aligned} \rho(\varepsilon)d\varepsilon &= \int_{V^*(\varepsilon)} \frac{(dp)^d (dr)^d}{h^d} \\ &\propto h^{-d} \int_0^{r^*(\varepsilon)} p^{d-1} dp r^{d-1} dr \\ &= \left(\frac{h^2}{2m}\right)^{-d/2} \int_0^{r^*(\varepsilon)} \sqrt{(\varepsilon - U(r))^{d-2}} r^{d-1} dr d\varepsilon \end{aligned} \quad (48)$$

where $V^*(\varepsilon)$ is the volume available for the system at the energy ε , and r^* is defined by $U(r^*) = \varepsilon$. Choosing a power-law potential $U(r) = (h^2/mr_0^2)(r/r_0)^n$, we immediately obtain:

$$\rho(\varepsilon)d\varepsilon \approx \left(\frac{r_0}{\Lambda}\right)^{2\eta} \left(\frac{\varepsilon}{kT}\right)^{\eta-1} \frac{d\varepsilon}{kT} \quad (49)$$

with $\eta = d/2 + d/n$. From Eqs. 49 and 47 the scaling law for the critical temperature T_c can be found by taking $N_0 = 0$ and $\mu = 0$:

$$kT_c \propto \frac{h^2}{mr_0^2} \left[\frac{N}{I}\right]^{1/\eta} \quad (50)$$

Equation 50 also gives us the ground-state population fraction for $T < T_c$:

$$\frac{N_0}{N} = 1 - (T/T_c)^\eta \quad (51)$$

reproducing the 3D special case of Eq. 7. Thus the deeper the potential well (i.e., the higher the value of h^2/mr_0^2), the higher the value of T_c . The “confinement power” of the potential, defined as $-N^{-1}T_c(dN_0/dT)_{T=T_c} = \eta$ [18], can be seen to depend on the shape of the potential but not on its strength. The integral in Eq. 50:

$$I = \int_0^\infty \frac{x^{\eta-1} dx}{e^x - 1} \quad (52)$$

is equal to $\Gamma(\eta)\zeta(\eta)$ for $\eta > 1$ and diverges otherwise. Thus the condition for BEC ($T_c > 0$) in thermodynamic limit (see below) is given by:

$$d > \frac{2n}{n+2} \quad (53)$$

We see that an ideal Bose gas confined in a box ($n \rightarrow \infty$) displays BEC only in 3D [14–16]. In a harmonic potential, ($n = 2$) the BEC condition can be fulfilled only in 3D or 2D [19].

It can be also shown [18] that the heat capacity $C(T)$ [The heat capacity is defined by $C(T) = \partial E(T)/\partial T$ with the total energy of the system given by $E(T) = \int_0^\infty \varepsilon N_\varepsilon \rho(\varepsilon) d\varepsilon$.] is discontinuous at T_c for $d/n + d/2 > 2$. If $d/n + d/2 \leq 2$, $C(T)$ is continuous at T_c , but $\partial C(T)/\partial T$ is discontinuous. In general, $C(T)$ is larger for a power-law potential than for a rigid wall container. This is because increasing the energy of the gas requires work against the confining potential.

BEC in a Finite System

The reason of the ‘‘BEC failure’’ for $\eta \leq 1$ must be found in the usual thermodynamic limit, which assumes $N \rightarrow \infty$ and $r_0 \rightarrow \infty$ with $N/r_0^{2\eta}$ finite. For a real system of finite size the lower limit divergence in Eq. 52 is unphysical. Let us consider a particular case $\eta = 1$ corresponding to a 1D harmonic potential and also to a 2D box. Introducing E_1/kT as the lower limit of the integral Eq. 52 with E_1 of the order of the first excited state, we obtain for the transition temperature [the exact results [7] are: $E_1 = \hbar\omega/2$ for a 1D-harmonic potential and $E_1 = \hbar^2/(8Mr_0^2)$ for a 2D box]:

$$N \propto \frac{kT_c}{E_1} \ln \left(\frac{kT_c}{E_1} \right) \quad (54)$$

and for the condensate fraction:

$$\frac{N_0}{N} = 1 - \frac{T \ln(kT/E_1)}{T_c \ln(kT_c/E_1)} \quad (55)$$

with the logarithmic terms becoming negligible for large particle number in accordance with Eq. 51 for $\eta = 1$. Thus the predicted impossibility of BEC in low-dimensional systems is an artifact of the thermodynamic limit, which does not apply to the situation realized in atoms traps.

The N -finite effects are less dramatic for systems showing BEC in the thermodynamic limit ($\eta > 1$). As an illustration let us consider a 3D harmonic potential ($\eta = 3$ and $r_0^2 = \hbar/m\omega$) whose BEC condition (Eq. 50) takes the form:

$$N \sim \left(\frac{kT_c}{\hbar\omega} \right)^3 \quad (56)$$

Obviously, this is the first term of the expansion in large parameter $kT/\hbar\omega$ (see above). The next term should scale as $(kT/\hbar\omega)^2$, giving us the first correction to the critical temperature:

$$\frac{T_c^0 - T_c}{T_c^0} \sim N^{-1/3} \quad (57)$$

An exact calculation [7] shows that for $N = 10^3$ the transition temperature T_c is less than 7% the usual result T_c^0 extrapolated from $N = \infty$. It is interesting to rewrite Eq. 50 as:

$$N \sim \left(\frac{kT_c}{U_0} \right)^{d/n} r_0^d \left(\frac{MkT_c}{\hbar^2} \right)^{d/2} \quad (58)$$

Introducing an effective volume $V^* \sim r^d$ of the system which is determined by $kT \sim U_0(r/r_0)^n$, that is, $V^* \sim r_0^d (kT/U_0)^{d/n}$ and using for the de Broglie wavelength $\Lambda^2 \sim \hbar^2/MkT$, we obtain the general condition for quantum degeneracy:

$$\Lambda^d \frac{N}{V^*} \sim 1 \quad (59)$$

1. Einstein A (1924, 1925) Sitzungberichte, Preussische Akademie der Wissenschaften, Berlin. 1924:261–267; 1925:3–14
2. Bose SN (1924) Z. Phys. 26:178
3. Landau LD, Lifschitz EM (1958) Statistical physics, 1st edn., Pergamon, London
4. Greytak TJ, Kleppner D (1984) In: Grynberg G, Stora R (eds) New trends in atomic physics. North-Holland, Amsterdam
5. Arimondo E, Phillips WD, Strumia F (eds) (1992) Laser manipulation of atoms and ions. North-Holland, Amsterdam
6. Hess H (1986) Phys. Rev. B34:3476
7. Ketterle W, van Druten NJ (1996) In: Bederson B, Walther H (eds) Advances in atomic, molecular and optical physics, vol. 37. Academic Press, Cambridge, p. 181
8. Anderson MH, et al. (1985) Science 269:198
9. Ensher JR, et al. (1996) Phys Rev Lett 77:4984
10. Davis KB, et al. (1995) Phys Rev Lett 75:3969
11. Mewes M-O, et al. (1996) Phys Rev Lett 77:988
12. Bradley CC, et al. (1995) Phys Rev Lett 75:1687;
13. Bradley CC, Sackett CA, Hulet RG (1997) Phys Rev Lett 78:985
14. Hohenberg PC (1967) Phys Rev 158:383
15. Mermin ND, Wagner H (1966) Phys Rev Lett 17:1133
16. Mermin ND (1968) Phys Rev 176:250
17. Widom A (1968) Phys Rev 176:254
18. Bagnato V, Pritchard DE, Kleppner D (1987) Phys Rev A35:4354
19. Bagnato V, Kleppner D (1991) Phys Rev A44:7439
20. Ketterle W, van Druten NJ (1996) Phys Rev A54:656
21. Kosterlitz JM, Thouless DJ (1973) J Phys C6:1181

22. Julienne PS, Smith AM, Burnett K (1993) In: Bates DR, Bederson B (eds) *Advances in atomic, molecular and optical physics*, vol. 30. Academic, San Diego, pp 141–198
23. Gardiner JR, et al. (1995) *Phys Rev Lett* 74:3764
24. Tiesinga E, et al. (1996) *J Res Natl Inst Stand Technol* 101:505
25. Abraham E, et al. (1995) *Phys Rev Lett* 74:1315
26. Sackett CA, et al. (1997) *Appl Phys B*65:433
27. Gross EP (1961) *N Cim* 20:454
28. Gross EP (1963) *J Math Phys* 4:195
29. Pitaevsky LP (1961) *Sov Phys JEPT* 13:451
30. Stringari S (1996) *Phys Rev Lett* 77:2360
31. Jin DS, et al. (1996) *Phys Rev Lett* 77:420
32. Mewes M-O, et al. (1996) *Phys Rev Lett* 77:416
33. Edwards M, et al. (1996) *Phys Rev Lett* 77:1671
34. Singh KG, Rokhsar DS (1996) *Phys Rev Lett* 77:1667
35. Andrews MR, et al. (1996) *Science* 273:84
36. Peierls R (1979) *Surprises in theoretical physics*. Princeton University Press, Princeton
37. Loudon R (1984) *The quantum theory of light*. Clarendon, Oxford
38. Andrews MR, et al. (1997) *Science* 275:637
39. Röhrl A, Naraschewski M, Schenzle A, Wallis H (1997) *Phys Rev Lett* 78:4143
40. Mandel L, Wolf E (1995) *Optical coherence and quantum optics*. Cambridge University Press, Cambridge
41. Ketterle W (1999) *Atom laser*. In: McGraw-Hill 1999 Yearbook of Science & Technology. McGraw-Hill, New York
42. Penrose O, Onsager L (1956) *Phys Rev* 104:576
43. Anderson PW (1984) *Basic notions of condensed matter physics*. Benjamin, London
44. Ho TL, Ma M (1997) cond-mat./9703034 v2
45. Monien H, Linn M, Elstner N (1998) *Phys Rev Lett* (submitted)